PALEOCEANOGRAPHY, VOL. 20, PA4005, doi:10.1029/2004PA001061, 2005

Last deglaciation in the Okinawa Trough: Subtropical northwest Pacific link to Northern Hemisphere and tropical climate

Youbin Sun,[1,2] Delia W. Oppo,[3] Rong Xiang,[4] Weiguo Liu,[5] and Shu Gao[6]

Received 16 June 2004; revised 31 May 2005; accepted 23 June 2005; published 7 October 2005.

[1] Detailed deglacial and Holocene records of planktonic $\delta^{18}O$ and Mg/Ca–based sea surface temperature (SST) from the Okinawa Trough suggest that at ~18 to 17 thousand years before present (kyr B.P.), late spring/early summer SSTs were approximately 3°C cooler than today, while surface waters were up to 1 practical salinity unit saltier. These conditions are consistent with a weaker influence of the summer East Asian Monsoon (EAM) than today. The timing of suborbital SST oscillations suggests a close link with abrupt changes in the EAM and North Atlantic climate. A tropical influence, however, may have resulted in subtle decoupling between the North Atlantic and the Okinawa Trough/EAM during the deglaciation. Okinawa Trough surface water trends in the Holocene are consistent with model simulations of an inland shift of intense EAM precipitation during the middle Holocene. Millennial-scale alternations between relatively warm, salty conditions and relatively cold, fresh conditions suggest varying influence of the Kuroshio during the Holocene.

Citation: Sun, Y., D. W. Oppo, R. Xiang, W. Liu, and S. Gao (2005), Last deglaciation in the Okinawa Trough: Subtropical northwest Pacific link to Northern Hemisphere and tropical climate, *Paleoceanography*, *20*, PA4005, doi:10.1029/2004PA001061.

1. Introduction

[2] Seasonal variations in wind, rain, and temperature associated with the Austral-Asian monsoon systems affect a vast expanse of tropical and subtropical Asia. The seasonal monsoon reversals are driven by the annual cycle of insolation and its effect on the land-sea thermal contrast. Interannual variability in monsoon intensity is also linked to interannual variability in the tropical Pacific, namely, the El Niño–Southern Oscillation (ENSO). This is particularly the case for the coupled tropical northwest Pacific Monsoon (NWM) and the subtropical East Asian Monsoon (EAM) affecting East Asia, and less so for the Indian monsoon [*Wang et al.*, 2003]. Interannual variability in Eurasian snow cover may also influence the intensity of the Asian monsoons [e.g., *Barnett et al.*, 1989]. On glacial-interglacial and suborbital timescales, abundant evidence documents a strong link between the EAM and high-latitude Northern Hemisphere climate [e.g., *Porter and An*, 1995; *An*, 2000; *Wang et al.*, 2001].

[3] Deglacial oscillations in the EAM intensity were tightly coupled to variations in the North Atlantic region, exhibiting abrupt changes coeval with the Bølling-Allerød (BA) and Younger Dryas (YD) [*Wang et al.*, 1999; *Zhou et al.*, 2001; *Wang et al.*, 2001]. Although the hydrology of the western and eastern near-equatorial Pacific appeared linked to North Atlantic climate during deglaciation [*Rosenthal et al.*, 2003], the sea surface temperature (SST) signal is more complex [*Kiefer and Kienast*, 2005]. Marginal basins such as the South China Sea (SCS) exhibit a North Atlantic SST signature, attesting to a strong continental influence [e.g., *Wang et al.*, 1999; *Kienast et al.*, 2001]. By contrast, significant sustained SST oscillations, synchronous with the YD or Antarctic Cold Reversal (ACR) are absent, or not yet documented, in regions under weaker monsoonal influence, such as the Sulu Sea [*Rosenthal et al.*, 2003] and Indonesian region [*Visser et al.*, 2003; *Stott et al.*, 2004].

[4] The goal of this study was to develop detailed surface records from the northwestern subtropical Pacific, in a region that is under the strong influence of the EAM today and is also linked to the tropics via the Kuroshio Current. We present $\delta^{18}O$ and Mg/Ca–based SST records of the surface dwelling planktonic foraminifer *Globigerinoides ruber* (*G. ruber*) from the middle Okinawa Trough spanning the past 17–18 kyr and address the potential linkages to climate changes in the North Atlantic and western tropical Pacific.

2. Oceanographic Setting

[5] The Okinawa Trough, as the southeastern part of the East China Sea, is a typical curved basin behind the Ryukyu Arc of the northwestern Pacific (Figure 1). Today, the surface hydrography of the Okinawa Trough is strongly influenced by the EAM. The alternation between cold, dry winter monsoon winds and warmer moist summer monsoon winds influences surface heat fluxes in the western Pacific, having a mean seasonal range of ~300 W/m^2 in the vicinity

[1]Department of Earth Sciences, Institute of Surficial Geochemistry, Nanjing University, Nanjing, China.
[2]Now at Department of Earth and Planetary Science, University of Tokyo, Tokyo, Japan.
[3]Department of Geology and Geophysics, Woods Hole Oceanographic Institution, Woods Hole, Massachusetts, USA.
[4]Key Laboratory of Marginal Sea Geology, South China Sea Institute of Oceanology, Chinese Academy of Sciences, Gangzhou, China.
[5]State Key Laboratory of Loess and Quaternary Geology, Institute of Earth Environment, Chinese Academy of Sciences, Xi'an, China.
[6]Ministry of Education Key Laboratory of Coast and Island Development, Nanjing University, Nanjing, China.

0883-8305/05/2004PA001061$12.00

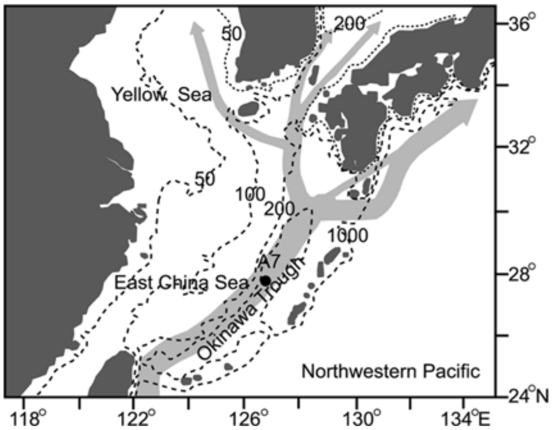

Figure 1. Location of core A7 in the middle Okinawa Trough. Shaded arrows indicate the Kuroshio Current and its branches, and dashed lines are the isobaths.

of the Okinawa Trough [*Qiu et al.*, 2004]. The path and volume transport of the Kuroshio Current, which originates from the North Equator Current (NEC) and carries warm and saline water flowing northeastward along the edge of the East China Sea continental shelf, are also influenced by the EAM. Monsoonal winds determine the latitude of the bifurcation point of the NEC, which in turn determines the volume of water originating in the NEC that enters the Luzon Strait into the South China Sea versus the volume that flows poleward in the Kuroshio Current [*Kagimoto and Yamagata*, 1997; *Qu and Lukas*, 2003; *Qu et al.*, 2004]. A southern position of the NEC bifurcation during the summer monsoon season favors poleward transport of tropical waters in the Kuroshio Current whereas a northerly position of the NEC bifurcation during the winter monsoon season favors less transport in the Kuroshio Current.

[6] Seasonal SSS variability in the Okinawa Trough is also driven by monsoon-related processes, with fresher summer surface waters reflecting the greater influx of runoff from the Huanghe (Yellow) and Changjiang (Yangtze) Rivers. Lower salinity in summer than winter (Figure 2) indicates that monsoon runoff dominates over seasonal changes in the Kuroshio Current, whose effect is to increase the salinity in summer, when its transport is greatest. Climatological mean annual SSTs near the Okinawa Trough core site are ~24°C, with a maximum in August (28.9°C) and minimum in February (20°C). Mean annual sea surface salinity (SSS) averages 34.3 practical salinity units (psu), with a minimum in July (33.7 psu) and maximum in January (34.7 psu) [*Levitus and Boyer*, 1994].

[7] Pacific interannual variability may also influence surface conditions in the Okinawa Trough through its influence on the NEC bifurcation latitude and Kuroshio transport. Kuroshio Current transport is weakened during El Niño years and strengthened during La Niña years, but today the effect of interannual variability is secondary to the seasonal cycle of volume transport driven by monsoon winds [*Kim et al.*, 2004; *Qu et al.*, 2004].

[8] The existence of a land bridge connecting the southern Ryukyu Arc to Taiwan during the Last Glacial Maximum (LGM), which may have prevented the Kuroshio Current from entering the Okinawa Trough, has been inferred from planktonic foraminiferal assemblages changes [*Ujiié et al.*, 1991; *Ujiié and Ujiié*, 1999; *Ujiié et al.*, 2003]. Consequently, and as a result of lower sea level, coastal waters may have had a greater influence on surface waters in the trough [*Xu and Oda*, 1999]. However, our data, discussed below, indicate the continued influence of salty Pacific waters throughout our study interval.

3. Materials and Methods

[9] Gravity core A7 (126°58.7′E, 27°49.2′N), 4.5 m in length, was retrieved from the middle Okinawa Trough at a water depth of 1264 m (Figure 1). Core A7 consists of gray silty clay with an ash layer at 1.02–1.10 m and several small turbidites whose extent is well constrained by sedimentological analysis [*Sun et al.*, 2003]. The ash layer likely corresponds to the widespread tephra erupted from southern Kyushu in Japan (hereafter referred to as K-Ah tephra) [*Machida and Arai*, 1978], which has been identified previously in the middle Okinawa Trough [*Li et al.*, 2001]. The tephra was deposited at ~7.3 calendar (cal.) kyr B.P. as indicated by both the AMS ^{14}C dating of terrestrial macrofossils and varve counts of the sedi-

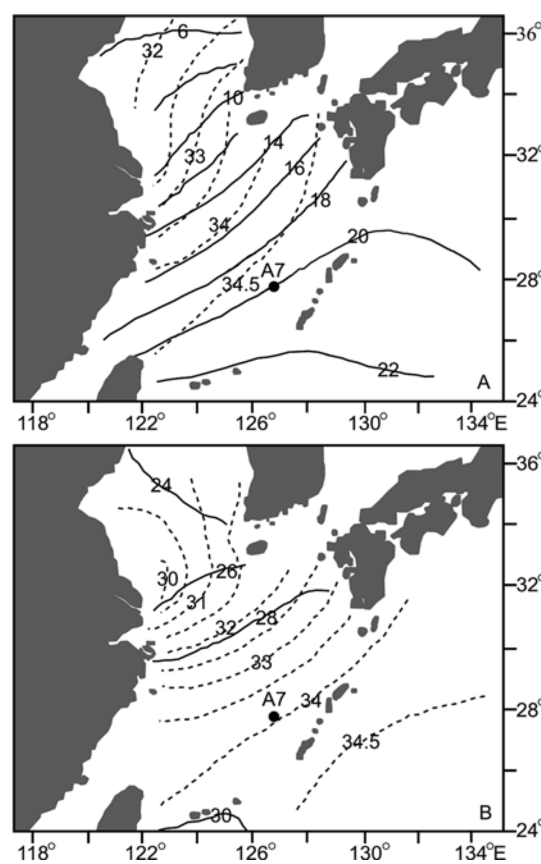

Figure 2. Okinawa Trough climatological sea surface temperature (SST) and salinity (SSS) for February (a) and August (b) [*Levitus and Boyer*, 1994]. Solid and dashed lines denote the contours of SST and SSS, respectively.

Table 1. AMS Radiocarbon and Calendar Ages for Core A7[a]

Accession Number	Depth, m	AMS ^{14}C Age, years B.P.	AGE1 Calendar Years B.P.	AGE1 2σ Error Bars, years	AGE2 Calendar Years B.P.	AGE2 2σ Error Bars, years
OS-45820	0.02–0.06	1910 ± 30	1,450	1366, 1536	1,160	1083, 1255
OS-39785	0.32–0.36	2890 ± 35	2,690	2528, 2744	2,300	2151, 2338
OS-45821	0.64–0.68	4800 ± 35	5,040	4951, 5243	4,700	4575, 4808
OS-39786	0.94–0.98	6860 ± 45	7,400	7275, 7461	7,100	6948, 7199
OS-39858	1.20–1.22	8420 ± 45	9,000	8905, 9198	8,580	8452, 8743
OS-39859	1.44–1.46	9030 ± 65	9,700	9524, 9955	9,420	9254, 9519
OS-39860	1.74–1.76	10500 ± 60	11,700	11354, 11927	11,190	11105, 11304
OS-39861	2.04–2.06	10800 ± 65	12,300	12009, 12625	11,700	11341, 11935
OS-45822	2.22–2.26	10850 ± 45	12350	12116, 12639	11900	11412, 11994
OS-39862	2.58–2.60	11450 ± 70	12940	12870, 13096	12800	12662, 12874
OS-45823	2.86–2.90	12200 ± 50	13680	13483, 13776	13320	13242, 13436
OS-39863	3.20–3.24	12850 ± 60	14400	14176, 14886	14000	13838, 14142
OS-45824	3.46–3.50	13300 ± 55	15200	14981, 15515	14880	14459, 15120
OS-39864	3.70–3.74	13650 ± 75	15680	15322, 16107	15260	15003, 15627
OS-39865	4.42–4.46	15200 ± 90	18000	17569, 18525	17550	16956, 17902

[a]AGE1 uses ages estimated from calibration curve MARINE04 [*Hughen et al.*, 2004] with a 400-year reservoir age. AGE2 uses a 700-year reservoir age.

ments in Lake Suigetsu [*Kitagawa et al.*, 1995; *Fukusawa*, 1995].

[10] Two hundred twenty-five samples were taken at 2-cm intervals and wet washed through a 63-μm sieve. About 40 shells of *G. ruber* were picked from the 250- to 355-μm size fraction for oxygen isotope and Mg/Ca analyses. Sediment trap data indicate that the flux of *G. ruber* in the western subtropical Pacific occurs throughout the year [*Yamasaki and Oda*, 2003], possibly peaking in June and July, with smaller or less consistent peaks in spring (April) and winter (December/January) [*Mohiuddin et al.*, 2002]. Sediment trap data from the central subtropical Pacific showing peak fluxes in September, shortly after the August SST maximum, clearly indicate *G. ruber's* preference for warm, stratified waters [*Eguchi et al.*, 2003].

[11] Oxygen isotope analyses were performed using a Finnegan-MAT-252 mass spectrometer at the Institute of Earth Environment, the Chinese Academy of Sciences. The precision of the measurements is better than ±0.06‰ for $\delta^{18}O$, as determined by replicate analyses of NBS-19 and laboratory standards (PTB-1). For Mg/Ca analysis, approximately 300 μg of *G. ruber* (25 shells) were weighed, gently crushed, and cleaned using a multistep reductive/oxidative procedure developed for trace element analysis [*Boyle and Keigwin*, 1985]. The Mg/Ca ratio was determined on a Finnegan Element-2 inductively coupled plasma–mass spectrophotometer (ICP-MS) at the Woods Hole Oceanographic Institution. On the basis of determinations of three different consistency standards, internal reproducibility of Mg/Ca is estimated to be better than 5%. Sixteen samples were repicked and rerun because the original measurements fell off trends defined by neighboring high-resolution samples. The standard error of the difference of these analyses is ~0.08 mmol/mol, or ~0.25°C. Thus we conservatively estimate the total measurement error to be equivalent to ~±0.5°C.

[12] About 20 mg of planktonic foraminifer *Neogloboquadrina dutertrei* shells (>150 μm) were picked from 15 horizons and dated at the National Ocean Sciences Accelerator Mass Spectrometry (AMS) Facility, the Woods Hole Oceanographic Institution, USA.

4. Results

4.1. Age Models

[13] All AMS ^{14}C ages were first converted to calendar years using the Calib 5.0 program (available at http://radiocarbon.pa.qub.ac.uk/calib/) utilizes an updated calibration curve, MARINE04, [*Stuiver et al.*, 1998; *Hughen et al.*, 2004] and a 400-year surface-ocean reservoir correction [*Bard*, 1988] (AGE1). To construct our age model, we chose ages that occurred within maxima of the calendar age probability function. When more than one maximum occurred or a maximum was broad, we chose an age that minimized abrupt sedimentation rate changes (Table 1, Figure 3, and AGE1). Linear interpolation between dated levels above and below the K-Ah ash layer gives a 7.6 cal. kyr B.P. age for the top of the ash layer of estimated 7.3 cal.

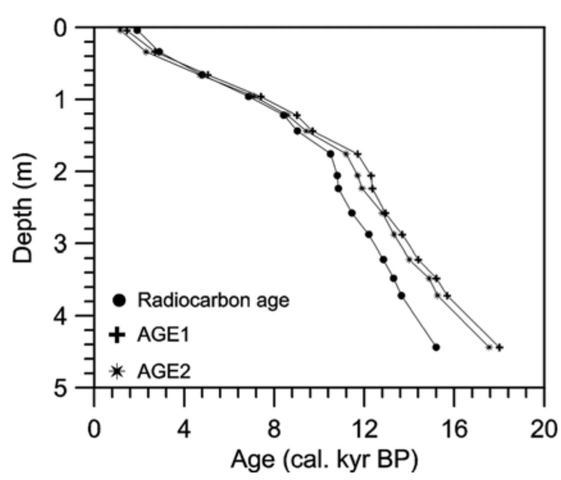

Figure 3. Radiocarbon and calendar ages versus depth in core A7. For calendar ages of the two age models and the ~95% confidence interval, see Table 1.

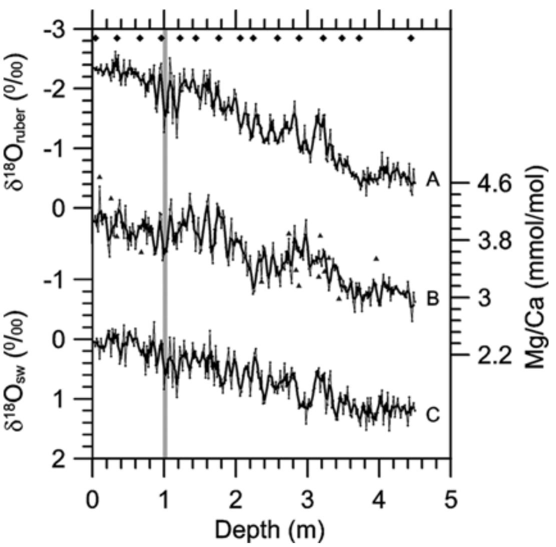

Figure 4. The (a) $\delta^{18}O$ record and (b) Mg/Ca ratio of *G. ruber* and (c) $\delta^{18}O_{sw}$ versus depth in core A7. Rejected Mg/Ca analyses are shown as triangles, and a shaded bar indicates the position of the ash layer. Diamonds show the positions of the AMS ^{14}C dating. Bold lines indicate three-point running mean plotted in Figures 5 and 6.

kyr B.P. age, suggesting that the 400-year reservoir correction is too small for the Holocene. We thus recalibrated the radiocarbon dates using a 700-year reservoir age (Table 1, Figure 3, and AGE2). Estimates of surface reservoir age in the westernmost Okinawa Trough, however, are close to the 400-year global mean or smaller [*Reimer et al.*, 2004] (see http://radiocarbon.pa.qub.ac.uk/marine/), but are higher to the north, off eastern Japan. While we prefer AGE2 because it gives closer agreement with the ash age, we believe the two age models provide a reasonable range of ages for the down-core records. An additional caveat, however, is that variations in atmospheric radiocarbon production and changes in the global carbon cycle result in large uncertainties during some intervals [e.g., *Hughen et al.*, 1998, 2000]; the 2-sigma (95% confidence level) error bars on the ages provided by the Calib 5.0 usually exceeded several hundred years (Table 1).

[14] In summary, as is true of most other radiocarbon-dated marine records spanning the deglaciation, there exists considerable uncertainty in the chronology due both to the uncertainties in the calibration and to the possibility of variable reservoir age. These age models suggest that sediment accumulation rates vary from an average of ~40 cm/kyr during deglaciation to an average of ~15 cm/kyr during the Holocene.

4.2. Early Deglacial-Holocene Differences

[15] A radiocarbon-based calendar age of ~17–18 kyr B.P. (Table 1) near the bottom of the core indicates that the corer did not fully penetrate glacial maximum sediments (18–24 cal. kyr B.P.), as recently defined by *Mix et al.* [2001]. Hence we refer to the interval of time represented by core bottom values (~17–18 cal. kyr B.P.) as the "early deglacial," consistent with the observation that gradual sea level rise had already begun [*Fairbanks*, 1989]. The planktonic $\delta^{18}O_{ruber}$ record exhibits a 1.7‰ decrease from ~17 cal. kyr B.P. to the Holocene (Figure 4a). This decrease includes 0.95‰ of the full 1‰ effect of ice volume change [*Schrag et al.*, 1996] and local SST and SSS change.

[16] The contribution to $\delta^{18}O_{ruber}$ due to SST is estimated using the Mg/Ca–based SST reconstruction. Mg/Ca varied from a maximum of 4.55 mmol/mol to a minimum of 2.67 mmol/mol (Figure 4b). Many calibrations exist for converting Mg/Ca to SST, with recent ones taking into consideration the potential effect of dissolution [*Rosenthal and Lohmann*, 2002]. In core A7, the average shell weight was almost constant, varying only between 11 and 13.5 μg (not shown). The lack of a trend over the length of the record reflects the position of the core (1264 m) well above the present carbonate lysocline (~1600 m). Hence the *G. ruber* Mg/Ca values were converted to SST using an equation developed from South China Sea core top sediment: $SST = \ln(Mg/Ca/0.38)/0.089$ [*Hastings et al.*, 2001], yielding a core top temperature of 26.6°C. The core top value is ~2° colder than peak summer (August) SST, but close to the average of June and July SST (26.8°C), when maximum fluxes of *G. ruber* seem to occur in the subtropical northwestern Pacific [*Mohiuddin et al.*, 2002]. Accordingly, we interpret down-core SST changes to reflect changes in summer SST, with a slight colder season bias. At colder times in the past, it is possible that the maximum flux of *G. ruber* shifted to the warmest month, implying that down-core SST variations underestimate the true amplitude of variability. Application of the preservation-dependent calibration of *Rosenthal and Lohmann* [2002], which was developed for smaller *G. ruber* shells (212–300 μm) than those used in this study (250–350 μm) yields SST estimates that are ~0.5°C warmer than those reported here, but does not significantly change our results. The early deglacial summer SSTs were approximately 3°C cooler than the late Holocene, and ~0.5°C higher than the warm season faunal SST estimates from nearby core DGKS9603 [*Li et al.*, 2001].

[17] The early deglacial-Holocene amplitude of surface water $\delta^{18}O$ ($\delta^{18}O_{sw}$) (Figure 4c), ~1.3‰, estimated from paired $\delta^{18}O_{ruber}$ and Mg/Ca–based SST, includes a 0.95‰ change due to global ice volume change, which had already begun, and a ~0.35‰ residual. The sea level component is removed from the $\delta^{18}O_{sw}$ record using the Barbados sea level curve [*Fairbanks*, 1989] and a 1‰ mean ocean $\delta^{18}O$ change [*Schrag et al.*, 1996]. The residual ($\delta^{18}O_{resid}$) (Figure 5c) reflects only $\delta^{18}O_{sw}$ changes due to local salinity variability or changes in the $\delta^{18}O$ of runoff. On the basis of ongoing measurements of seawater salinity and $\delta^{18}O_{sw}$ in the southern Okinawa Trough, a 1‰ $\delta^{18}O_{sw}$ decrease corresponds to a salinity decrease of approximately 1 psu [*Lin*, 2005]. Thus, if the modern relationship was applicable to past changes, the 0.35‰ $\delta^{18}O_{resid}$ change suggests that early deglacial SSS was ~0.7 psu higher than today. Although the site of A7 was located closer to land and under greater influence of fresh coastal waters during times of lower sea level stand, the weakening of the summer monsoon and attendant runoff may have compensated for

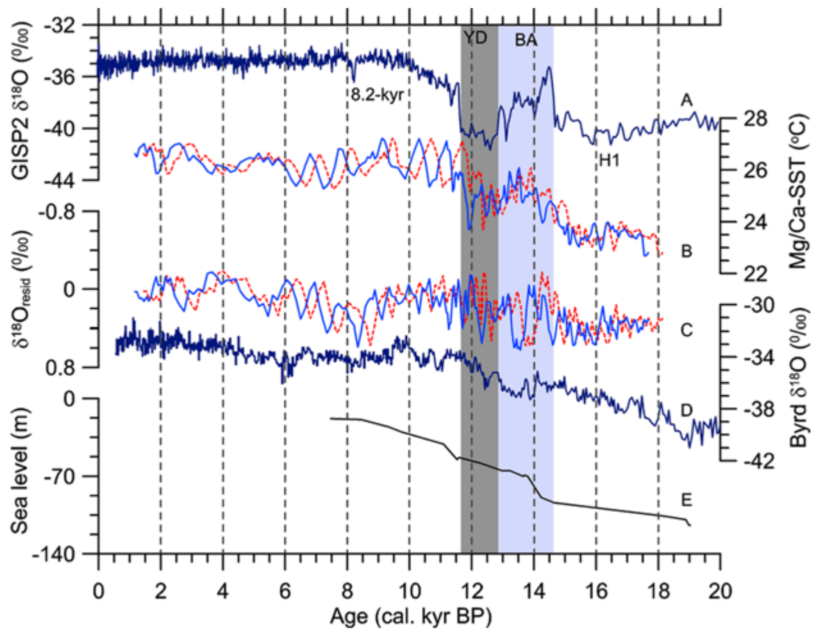

Figure 5. Comparison of climate records from Antarctica, Okinawa Trough, and Greenland. (a) The $\delta^{18}O$ record of GISP2 ice core [*Stuiver and Grootes*, 2000]. (b) Mg/Ca–based SST. (c) The $\delta^{18}O_{residual}$ record, estimated from paired $\delta^{18}O_{ruber}$ and Mg/Ca–based SST and removing global ice volume effects. (d) The $\delta^{18}O$ record of Byrd ice core [*Blunier et al.*, 1998]. (e) Barbados sea level curve [*Fairbanks*, 1989]. Solid and dashed lines on Figures 5b and 5c denote records on the AGE2 and AGE1 chronologies, respectively.

the closer proximity to shore, or the $\delta^{18}O$ value of monsoon-derived river runoff was somewhat more positive than today [*Hoffman and Heimann*, 1997].

4.3. Deglacial SST Oscillations

[18] Suborbital oscillations are superimposed on the deglacial SST rise (Figure 5b). The uncertainty in the age model does not preclude making general comments about the apparent timing of these oscillations. A minor cooling near ~16–15.5 kyr B.P. may be contemporaneous with North Atlantic Heinrich event 1 (H1), and a larger cooling centered near ~12.5 kyr B.P. appears contemporaneous with the North Atlantic Younger Dryas (YD) cold event (Figure 5a), both suggesting a strong link of Okinawa SSTs to the North Atlantic. However, the temporal SST pattern differs from the North Atlantic pattern in significant ways, suggesting some decoupling. Most notably, whereas the warmest pre-YD temperatures in the North Atlantic occurred early in the BA (~14.5 cal. kyr B.P.), SST continued to rise in the Okinawa Trough, peaking 500–1000 years later. SSTs subsequently dropped, culminating in peak cold during the first half of the YD, generally consistent with the GISP2 $\delta^{18}O$ record. Following minimum SSTs, the Okinawa Trough warmed dramatically, whereas Greenland exhibited only small and gradual climate amelioration. The end of the Younger Dryas in the Okinawa Trough was marked by an abrupt warming that occurred, within age model uncertainty, synchronously with Greenland warming. Large SST oscillations continued for the rest of the deglaciation and into the early Holocene, perhaps synchronously with relatively smaller North Atlantic oscillations documented by Greenland $\delta^{18}O$. Although not as well resolved, faunal (planktonic foraminifera) SST estimates from a nearby core in the Okinawa Trough show a similar deglacial warming trend, but suborbital variability was smaller [*Li et al.*, 2001].

[19] In summary, according to our age model and allowing for small age uncertainties, the deglacial SST temporal trends in the Okinawa Trough are consistent with a link to the North Atlantic region. From 12.5 to 10 cal. kyr B.P., however, one might equally well argue that the timing of SST oscillations was close to temperature trends in Byrd (Figure 5d), Antarctica. However, the closer timing of the deglacial cooling in the Okinawa Trough to the Younger Dryas than to the Antarctic Cold Reversal, on either age model, strongly suggests a closer link to northern hemisphere climate.

4.4. Deglacial $\delta^{18}O_{resid}$ Trends

[20] From ~16 to 14 cal. kyr B.P., warming was associated with decreasing $\delta^{18}O_{resid}$ values, or freshening, suggesting an increase in summer monsoon strength (Figure 5c). Peak deglacial warmth in the Okinawa Trough, however, was associated with a return to higher $\delta^{18}O_{resid}$ values. The association of peak warmth with an increase, rather than decrease, in $\delta^{18}O_{resid}$ values, indicates increased salinity, and is difficult to explain in the context of summer monsoon changes. However, after the return to fresher conditions (lower $\delta^{18}O_{resid}$ values) near the end of the Okinawa Trough warm peak, decreasing SSTs are generally associated with increasing $\delta^{18}O_{resid}$ values until ~13 cal. kyr B.P., consistent with a decrease in the influence of the summer EAM.

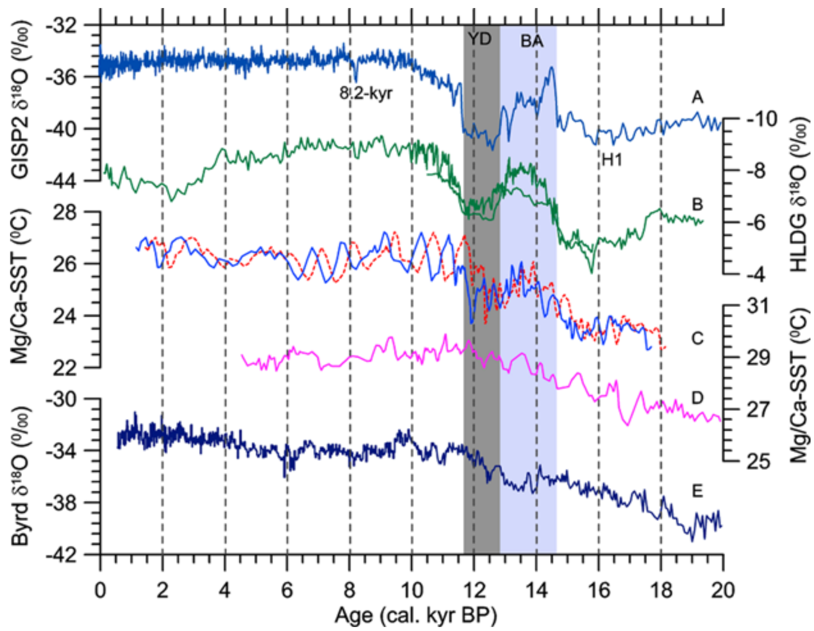

Figure 6. Comparison of SST records from the Okinawa Trough and the Sulu Sea with the $\delta^{18}O$ records from Hulu/Dongge caves and Byrd/GISP2 ice cores. (a) The $\delta^{18}O$ record of GISP2 ice core [*Stuiver and Grootes*, 2000]. (b) Stalagmite $\delta^{18}O$ record of Hulu/Dongge (HLDG) caves [*Wang et al.*, 2001; *Yuan et al.*, 2004]. (c) A7 SST. (d) Sulu Sea (MD97-2141) SST estimates [*Rosenthal et al.*, 2003]. (e) The $\delta^{18}O$ record of Byrd ice core [*Blunier et al.*, 1998]. A7 and MD97-2141 data were smoothed with a three-point running mean. Solid and dashed lines on (Figure 6c) denote records on the AGE2 and AGE1 chronologies, respectively.

The nature of the relationship between SST and $\delta^{18}O_{resid}$ variations changes from ~13 cal. kyr B.P., to ~9 cal. kyr B.P., when warm and saltier (increasing $\delta^{18}O_{resid}$ values) conditions alternate with cold and fresh (decreasing $\delta^{18}O_{resid}$ values).

4.5. The Holocene

[21] In core A7, maximum SSTs occurred during the late deglaciation/early Holocene (9–11.5 cal. kyr B.P.) and late (2.8–1.3 cal. kyr B.P.) Holocene, similar, although not necessarily related, to the longer-term Antarctic trend (Figure 5). SST oscillations (1.5°–2°C) occurred during the late deglaciation and Holocene, contrasting with faunal SST records from other Okinawa Trough cores suggesting that Holocene summer SSTs were relatively stable [*Jian et al.*, 2000; *Li et al.*, 2001]. A clear insolation-related trend of decreasing monsoon intensity since the early-middle Holocene, characteristic of terrestrial records from monsoon regions [e.g., *An*, 2000; *Fleitmann et al.*, 2003], is absent in this and other Okinawa Trough $\delta^{18}O$ records [*Jian et al.*, 2000] during the Holocene.

5. Discussion

5.1. The Deglaciation

[22] Monsoon forcing of the deglacial Okinawa Trough SST signal is supported by a comparison to the Hulu and Dongge Cave speleothem records (Figure 6b), which document changes in the relative intensity of summer and winter monsoon precipitation [*Wang et al.*, 2001; *Yuan et al.*, 2004]. These records indicate greater intensity of the summer monsoon relative to the winter monsoon at ~13 cal. kyr B.P. than at 14 cal. kyr B.P., similar to the SST pattern in the Okinawa Trough. Both the speleothem and Okinawa Trough records lack the saw-tooth temporal pattern characteristic of North Atlantic suborbital oscillations (Figure 6a). However, the deglacial SST rise and speleothem $\delta^{18}O$ decrease from about 16 to 14 cal. kyr B.P. occurred at approximately the same time as North Atlantic warming, with a SST jump corresponding to the onset of the BA warming. Thus the timing and amplitude of the Okinawa Trough SST record during the early part of the deglaciation, until the end of the Younger Dryas, suggests a dynamic link of the western subtropical Pacific to the North Atlantic via the EAM during the deglaciation (Figure 6). Dating uncertainties preclude determining whether subsequent deglacial SST oscillations in the Okinawa Trough were synchronous with EAM (speleothem) and North Atlantic (GISP2) oscillations, although such a correspondence is possible, as suggested by AGE2.

[23] As noted above, the $\delta^{18}O_{resid}$ record may provide some insight into the mechanisms for monsoonal control of Okinawa Trough SST. Cold and salty (positive $\delta^{18}O_{resid}$) surface waters from ~18–16 kyr B.P. are consistent with a weak summer monsoon during the late glaciation/early deglaciation. From ~16–14 cal. kyr B.P., a warming trend was associated with decreasing $\delta^{18}O_{resid}$ (decreasing salinity) suggesting a gradual strengthening of the summer monsoon. The association of warmth with freshening suggests that the intensification of the summer EAM controlled

the surface hydrography (see Figure 2). While warming continued from ~14 to 13.5 cal. kyr B.P., consistent with the further intensification of the summer monsoon, a dramatic increase in $\delta^{18}O_{resid}$ suggests a brief interval of increased salinity that cannot be easily explained.

[24] To assess the nature of the linkage between the Okinawa Trough and the tropics, we compare the Okinawa Trough SST record to the Mg/Ca–based SST record from the Sulu Sea [*Rosenthal et al.*, 2003], located between the southern SCS and the open western tropical Pacific. Like other western tropical Pacific sites less proximal to the Asian mainland than the SCS and Okinawa Trough [e.g., *Visser et al.*, 2003; *Stott et al.*, 2004], a strong deglacial cooling is not evident in the Sulu Sea, although small, brief, deglacial oscillations cannot be ruled out (Figure 6d). However, a tropical influence may have lead to the subtle decoupling between the North Atlantic and the EAM during deglaciation, such as the later peaking of the monsoon compared to North Atlantic temperatures during the BA (Figure 6).

[25] A significant implication of the absence of a large deglacial cooling event in the western tropical Pacific comparable to the YD suggests that while the tropics may have influenced the EAM, the EAM did not have a direct and clear influence tropical SST. The influence of the North Atlantic on monsoon climate seem to have dominated over tropical influences on land [*Wang et al.*, 2001], and in western Pacific marginal basins, including the Okinawa Trough and those to the south [*Kienast et al.*, 2001] and north [*Wang and Oba*, 1998; *Tada et al.*, 1999]. The similar timing of EAM rainfall and salinity anomalies in the Sulu Sea and eastern tropical Pacific [*Rosenthal et al.*, 2003], however, may indicate that the merging of EAM rainfall and rainfall in the western portion of Intertropical Convergence Zone (ITCZ) that occurs in the modern climate system [*Waliser and Gautier*, 1993] was also a feature of the deglaciation.

5.2. The Holocene

[26] The absence of a trend of declining SST and increasing $\delta^{18}O_{resid}$ since the early/mid Holocene contrasts with terrestrial evidence of declining summer EAM intensity over the course of the Holocene, suggesting a more complex response of the ocean to radiation forcing. In particular, the Okinawa Trough, in the subtropical North Pacific, may be influenced by water of both high- and low-latitude origin, which experienced opposing SST histories during the Holocene; the redistribution of solar radiation as a result of changing obliquity generally resulted in cooling of high-latitude waters and warming of tropical waters since the early Holocene [*Kitoh and Murakami*, 2002; *Liu et al.*, 2003]. The absence of a mid-Holocene minimum in $\delta^{18}O_{resid}$ (salinity) may also reflect a complex response to insolation forcing. For example, *Kitoh and Murakami* [2002], use an ocean-atmosphere general circulation model with 6 kyr B.P. insolation parameters, and simulate higher surface salinities in the western Pacific at 6 kyr B.P. relative to their control (0 kyr B.P.) simulation. The higher 6 kyr B.P. salinity is related to an inland shift of EAM precipitation, associated with a stronger summer EAM, relative to the control simulation. Our $\delta^{18}O_{resid}$ record suggesting no change (or possibly higher salinity) in the middle Holocene than late Holocene is consistent with the model simulations. Although monsoon precipitation at 6 kyr B.P. was higher on land, the westward shift in precipitation resulted in a net precipitation decrease in the western tropical and subtropical Pacific, as well as in most of coastal East Asia. Accordingly, in the mid-Holocene, the effect of greater EAM derived runoff from inland regions on salinity of the Okinawa rough was nearly balanced by a decrease in local precipitation and runoff derived from precipitation near the coast. Thus Holocene surface trends in the Okinawa Trough can be explained in the context of the response of the western subtropical Pacific to Holocene insolation change.

[27] Millennial oscillations are superimposed on the Holocene trend. The relationship between suborbital SST and $\delta^{18}O_{resid}$ oscillations during the late deglaciation and Holocene suggests a tropical influence on Okinawa Trough hydrography. The late deglaciation and Holocene are characterized by episodes of warm and salty (positive $\delta^{18}O_{resid}$) surface waters alternating with episodes of cold and fresh surface waters. The primary source of warm salty water is the Kuroshio Current, which brings water of tropical origin to Okinawa Trough. Thus oscillations within the Holocene may reflect variations in Kuroshio properties or its influence (northward transport in the Kuroshio). The observation that the amplitude of SST variability in the late deglacial/early Holocene was greater in the Okinawa Trough than in the western tropical Pacific (Sulu Sea) [*Rosenthal et al.*, 2003] (Figure 6d) suggests that changes in tropical SST were not solely responsible for the SST oscillations in the Okinawa Trough, but that variations in the influence of the Kuroshio may have also been involved.

[28] The main exception to the Holocene association of warmth with increased salinity and cold with freshening in the Okinawa Trough occurred from ~8.5 to 7.5 cal. kyr B.P., which probably corresponds to the broader cold event upon which the well-known North Atlantic 8.2 kyr B.P. event [e.g., *Alley et al.*, 1997] is superimposed. During this interval, estimated SST and $\delta^{18}O_{resid}$ suggest surface waters were colder and saltier, consistent with a weaker summer EAM.

6. Summary

[29] We have presented the first detailed deglacial records of planktonic $\delta^{18}O$ and Mg/Ca–based SST from the Okinawa Trough. The records indicate that at ~17–18 cal. kyr B.P., late spring/early summer SSTs were approximately 3°C cooler than today and surface waters were up to 1 psu saltier, consistent with a weak summer EAM.

[30] Significant SST oscillations in the Okinawa Trough are superimposed on the deglacial warming trend, and have a similar temporal pattern to variations in the seasonality of EAM precipitation. Although deglacial changes in the EAM precipitation and Okinawa Trough SST appear closely linked to climate variability in the North Atlantic region, tropical influence on the EAM is probably responsible for subtle differences between the North Atlantic and both the EAM and SST records during deglaciation.

[31] Paired SST and $\delta^{18}O_{resid}$ records may provide insights into the mechanisms of surface variability in the Okinawa Trough. During the early deglaciation, an increase of warm, fresh (coastal) surface water relative to cold, salty (northern subtropical) Pacific water suggests increasing summer monsoonal intensity. The absence of significantly fresher conditions in the western subtropical Pacific during the middle Holocene than late Holocene is consistent with an inland shift of the locus of intense EAM precipitation, as simulated by GCM experiments [e.g., *Kitoh and Murakami*, 2002]. Alternating warm, salty conditions with cold, fresh conditions suggests varying influence on millennial timescales of tropical (Kuroshio) waters during the late deglaciation and much of the Holocene.

[32] The overall picture that is emerging is that the North Atlantic influence on the EAM is particularly strong and extends to the Okinawa Trough and other western Pacific marginal basins [e.g., *Kiefer and Keinast*, 2005; *Wang et al.*, 1999] during the glacial and deglacial times, and during other particularly severe events such as the "8.2-kyr event." However, during these intervals of strong North Atlantic influence, tropical interactions decouple the EAM from the North Atlantic and influence SST patterns in the Okinawa Trough. Insolation-driven variations of the EAM influence Holocene surface trends in the Okinawa Trough. The tropics have an overriding influence on millennial-scale variability in the Okinawa Trough during the Holocene.

[33] **Acknowledgments.** We wish to thank the Institution of Oceanology, CAS and the crew of the R/V *Science I* for providing core A7 samples. We thank Rosemarie Came, Scot Birdwhistell, and Simon Thorold of WHOI for guidance during the Mg/Ca analyses. We are especially grateful to Markus Kienast, Thorsten Kiefer, and Konrad Hughen for insightful discussions on dating uncertainties and comments on the manuscript and for the critical review of an anonymous reviewer. Funding for this research was provided by NSFC (grants 40106006 and 40206007), SKLLQG (grant LLQG0204), and the NSF (OCE-020776 to DWO). Y.S.'s visit to WHOI was supported via a NSF START Fellowship. This is WHOI contribution number 11392.

References

Alley, R. B., P. A. Mayewski, T. Sowers, M. Stuiver, K. C. Taylor, and P. U. Clark (1997), Holocene climatic instability: A prominent, widespread event 8200 yr ago, *Geology*, *25*, 483–486.

An, Z. S. (2000), The history and variability of the east Asian paleomonsoon climate, *Quat. Sci. Rev.*, *19*, 171–187.

Bard, E. (1988), Correction of accelerator mass spectrometry ^{14}C ages measured in planktonic foraminifera: Paleoceanographic implications, *Paleoceanography*, *3*, 635–645.

Barnett, T. P., L. Dümenil, U. Schlese, E. Roeckner, and M. Latif (1989), The effect of Eurasian snow cover on regional and global climate variations, *J. Atmos. Sci.*, *46*, 661–685.

Blunier, T., et al. (1998), Asynchrony of Antarctic and Greenland climate change during the last glacial period, *Nature*, *394*, 739–743.

Boyle, E. A., and L. D. Keigwin (1985), Comparison of Atlantic and Pacific paleochemical records for the last 215,000 years: Changes in deep ocean circulation and chemical inventories, *Earth Planet. Sci. Lett.*, *76*, 135–150.

Eguchi, N. O., H. Ujiié, H. Kawahata, and A. Taira (2003), Seasonal variations in planktonic foraminifera at three sediment traps in the Subarctic, Transition and Subtropical zones of the central North Pacific Ocean, *Mar. Micropaleontol.*, *48*, 149–163.

Fairbanks, R. G. (1989), A 17,000-year glacio-eustatic sea level record: Influence of glacial melting rates on the Younger Dryas event and deep-ocean circulation, *Nature*, *342*, 637–642.

Fleitmann, D., S. J. Burns, M. Mudelsee, U. Neff, J. Kramers, A. Mangini, and A. Matter (2003), Holocene forcing of the Indian monsoon recorded in a stalagmite from southern Oman, *Science*, *300*, 1737–1739.

Fukusawa, H. (1995), Non-glacial varved lake sediment as a natural timekeeper and detector of environmental changes (in Japanese with English abstract), *Quat. Res. Tokyo*, *34*, 135–149.

Hastings, D., M. Kienast, S. Steinke, and A. A. Whitko (2001), A comparison of three independent paleotemperature estimates from a high resolution record of deglacial SST records in the tropical South China Sea, *Eos Trans. AGU*, *82*(47), Fall Meet. Suppl., Abstract PP12B-10.

Hoffman, G., and M. Heimann (1997), Water isotope modeling in the Asian monsoon region, *Quat. Int.*, *37*, 115–128.

Hughen, K. A., J. T. Overpeck, S. J. Lehman, M. Kashgarian, J. Southon, L. C. Peterson, R. Alley, and D. M. Sigman (1998), Deglacial changes in ocean circulation from an extended radiocarbon calibration, *Nature*, *391*, 65–68.

Hughen, K. A., J. R. Southon, S. J. Lehman, and J. T. Overpeck (2000), Synchronous radiocarbon and climate shifts during the last deglaciation, *Science*, *290*, 1951–1954.

Hughen, K. A., et al. (2004), MARINE04 marine radiocarbon age calibration, 0–26 cal kyr BP, *Radiocarbon*, *46*, 1059–1086.

Jian, Z. S., P. X. Wang, Y. Saito, L. J. Wang, U. Pflaumann, T. Oba, and X. R. Cheng (2000), Holocene variability of the Kuroshio Current in the Okinawa Trough, northwestern Pacific Ocean, *Earth Planet. Sci. Lett.*, *184*, 305–319.

Kagimoto, T., and T. Yamagata (1997), Seasonal transport variations of the Kuroshio: An OGCM simulation, *J. Phys. Oceanogr.*, *27*, 403–418.

Kiefer, T., and M. Kienast (2005), Patterns of deglacial warming in the Pacific Ocean: A review with emphasis on the time interval of Heinrich event 1, *Quat. Sci., Rev.*, *24*, 1063–1081.

Kienast, M., S. Steinke, K. Stattegger, and S. E. Calvert (2001), Synchronous tropical south China Sea SST change and Greenland warming during deglaciation, *Science*, *291*, 2132–2134.

Kim, Y. Y., T. Qu, T. Jensen, T. Miyama, H. Mitsudera, H.-W. Kang, and A. Ishida (2004), Seasonal and interannual variations of the North Equatorial Current bifurcation in a high-resolution OGCM, *J. Geophys. Res.*, *109*, C03040, doi:10.1029/2003JC002013.

Kitagawa, H., H. Fukusawa, T. Nakamura, M. Okamura, K. Takemura, A. Hayashida, and Y. Yasuda (1995), AMS ^{14}C dating of varved sediments from Lake Suigetsu, central Japan and atmospheric ^{14}C change during the late Pleistocene, *Radiocarbon*, *37*, 371–378.

Kitoh, A., and S. Murakami (2002), Tropical Pacific climate at the mid-Holocene and the Last Glacial Maximum simulated by a coupled ocean-atmosphere general circulation model, *Paleoceanography*, *17*(3), 1047, doi:10.1029/2001PA000724.

Levitus, S., and T. P. Boyer (1994), *World Ocean Atlas 1994*, vol. 4, *Temperature*, *NOAA Atlas NESDIS 4*, 129 pp., Natl. Oceanic and Atmos. Admin., Silver Spring, Md.

Li, T. G., Z. X. Liu, M. A. Hall, S. Berne, Y. Saito, S. X. Cang, and Z. B. Cheng (2001), Heinrich event imprints in the Okinawa Trough: Evidence from oxygen isotope and planktonic foraminifera, *Palaeogeogr. Palaeoclimatol. Palaeoecol.*, *176*, 133–146.

Lin, Y. S. (2005), Holocene paleoceanography in the upper reach of the Kuroshio, M.Sc. thesis, Natl. Taiwan Univ., Taiwan.

Liu, Z., E. Brady, and J. Lynch-Stieglitz (2003), Global ocean response to insolation forcing in the Holocene, *Paleoceanography*, *18*(4), 1041, doi:10.1029/2002PA000819.

Machida, H., and F. Arai (1978), Akahoya ash—A widespread marker erupted from Kikai caldera, southern Kyushu, Japan, *Quat. Res. Tokyo*, *17*, 143–163.

Mix, A. C., E. Bard, and R. R. Schneider (2001), Environmental processes of the ice age: Land, oceans, glaciers (EPILOG), *Quat. Sci. Rev.*, *20*, 627–657.

Mohiuddin, M. M., A. Nishimura, Y. Tanaka, and A. Shimamoto (2002), Regional and interannual productivity of biogenic components and planktonic foraminiferal fluxes in the northwestern Pacific basin, *Mar. Micropaleontol.*, *45*, 57–82.

Porter, S. C., and Z. S. An (1995), Correlation between climate events in the North Atlantic and China during the last glaciation, *Nature*, *375*, 305–308.

Qiu, B., S. Chen, and P. Hacker (2004), Synoptic-scale air–sea flux forcing in the western North Pacific: Observations and their impact on SST and the mixed layer, *J. Phys. Oceanogr.*, *34*, 2148–2159.

Qu, T., and R. Lukas (2003), The bifurcation of the North Equatorial Current in the Pacific, *J. Phys. Oceanogr.*, *33*, 5–18.
Qu, T., Y. Y. Kim, M. Yaremchuk, T. Tozuka, A. Ishida, and T. Yamagata (2004), Can Luzon Strait transport play a role in conveying the impact of ENSO to the South China Sea?, *J. Clim.*, *17*, 3644–3657.
Reimer, P. J., et al. (2004), IntCal04 terrestrial radiocarbon age calibration, 26–0 ka BP, *Radiocarbon*, *46*, 1029–1058.
Rosenthal, Y., and G. P. Lohmann (2002), Accurate estimation of sea surface temperatures using dissolution-corrected calibrations for Mg/Ca paleothermometry, *Paleoceanography*, *17*(3), 1044, doi:10.1029/2001PA000749.
Rosenthal, Y., D. W. Oppo, and B. K. Linsley (2003), The amplitude and phasing of climate change during the last deglaciation in the Sulu Sea, western equatorial Pacific, *Geophys. Res. Lett.*, *30*(8), 1428, doi:10.1029/2002GL016612.
Schrag, D. P., G. Hampt, and D. W. Murray (1996), The temperature and oxygen isotopic composition of the glacial ocean, *Science*, *272*, 1930–1931.
Stott, L., K. Cannariato, R. Thunell, G. H. Haug, A. Koutavas, and S. Lund (2004), Decline of western Pacific surface ocean salinity and temperature in the early Holocene, *Nature*, *431*, 56–59.
Stuiver, M., and P. M. Grootes (2000), GISP2 oxygen isotope ratios, *Quat. Res.*, *53*, 277–284.
Stuiver, M., P. J. Reimer, E. Bard, J. W. Beck, G. S. Burr, K. A. Hughen, B. Kromer, F. G. McCormac, J. van der Plicht, and M. Spurk (1998), INTCAL98 radiocarbon age calibration 24,000–0 cal BP, *Radiocarbon*, *40*, 1041–1083.
Sun, Y. B., S. Gao, and J. Li (2003), Preliminary analysis of grain-size populations with environmentally sensitive terrigenous materials in marginal sea setting, *Chin. Sci. Bull.*, *48*, 321–324.
Tada, R., T. Irino, and I. Koizumi (1999), Land-ocean linkages over orbital and millennial timescales recorded in late Quaternary sediments of the Japan Sea, *Paleoceanography*, *14*, 236–247.
Ujiié, H., and Y. Ujiié (1999), Late Quaternary course changes of the Kuroshio Current in the Ryukyu Arc region, northwestern Pacific Ocean, *Mar. Micropaleontol.*, *37*, 23–40.
Ujiié, H., Y. Tanaka, and T. Ono (1991), Late Quaternary paleoceanographic record from the middle Ryukyu Trench slope, northwestern Pacific, *Mar. Micropaleontol.*, *18*, 115–128.
Ujiié, Y., H. Ujiié, A. Taira, T. Nakamura, and K. Oguri (2003), Spatial and temporal variability of surface water in the Kuroshio source region, Pacific Ocean, over the past 21,000 years: Evidence from planktonic foraminifera, *Mar. Micropaleontol.*, *49*, 335–364.
Visser, K., R. Thunell, and L. Stott (2003), Magnitude and timing of temperature change in the Indo-Pacific warm pool during deglaciation, *Nature*, *421*, 152–155.
Waliser, D. E., and C. Gautier (1993), A satellite-derived climatology of the ITCZ, *J. Clim.*, *6*, 2162–2174.
Wang, B., S. C. Clemens, and P. Liu (2003), Contrasting the Indian and east Asian monsoons: Implications on geological timescales, *Mar. Geol.*, *201*, 5–21.
Wang, L., and T. Oba (1998), Tele-connections between east Asian Monsoon and the high-latitude climate: A comparison between the GISP 2 ice core record and the high resolution marine record from the Japan and the South China Sea, *Quat. Res. Tokyo*, *37*, 211–219.
Wang, L., M. Sarnthein, H. Erlenkeuser, J. Grimalt, P. Grootes, S. Heilig, E. Ivanova, M. Kienast, C. Pelejero, and U. Pflaumann (1999), East Asian monsoon climate during the late Pleistocene: High-resolution sediment records from the South China Sea, *Mar. Geol.*, *156*, 242–284.
Wang, Y. J., H. Cheng, R. L. Edwards, Z. S. An, Y. J. Wu, C. C. Shen, and J. A. Dorale (2001), A high-resolution absolute-dated late Pleistocene monsoon record from Hulu Cave, China, *Science*, *294*, 2345–2348.
Xu, X., and M. Oda (1999), Surface-water evolution of the eastern East China Sea during the last 36,000 years, *Mar. Geol.*, *156*, 285–304.
Yamasaki, M., and M. Oda (2003), Sedimentation of planktonic foraminifera in the East China Sea: Evidence from a sediment trap experiment, *Mar. Micropaleontol.*, *49*, 3–20.
Yuan, D. X., et al. (2004), Timing, duration, and transitions of the last interglacial monsoon, *Science*, *304*, 575–578.
Zhou, W. J., M. J. Head, Z. S. An, P. D. Deckker, Z. Y. Liu, X. D. Liu, X. F. Lu, D. Donahue, A. J. T. Jull, and J. W. Beck (2001), Terrestrial evidence for a spatial structure of tropical-polar interconnections during the Younger Dryas episode, *Earth Planet. Sci. Lett.*, *191*, 231–239.

S. Gao, Ministry of Education Key Laboratory of Coast and Island Development, Nanjing University, Nanjing 210093, China.

W. Liu, State Key Lab of Loess and Quaternary Geology, Institute of Earth Environment, Chinese Academy of Sciences, Xi'an 710054, China.

D. W. Oppo, Department of Geology and Geophysics, Woods Hole Oceanographic Institution, Woods Hole, MA 02543, USA. (doppo@whoi.edu)

Y. Sun, Department of Earth and Planetary Science, University of Tokyo, Hongo 7-3-1, Tokyo 113-0033, Japan. (youbin@eps.su-tokyo.ac.jp)

R. Xiang, Key Lab of Marginal Sea Geology, South China Sea Institute of Oceanology, Chinese Academy of Sciences, Gangzhou 510301, China.